PHYSICAL REVIEW D **96,** 055009 (2017)

Interpretation of the gamma-ray excess and AMS-02 antiprotons: Velocity dependent dark matter annihilations

Lian-Bao Jia*

School of Science, Southwest University of Science and Technology, Mianyang 621010, China
(Received 15 May 2017; published 11 September 2017)

The two messenger results of the GeV gamma-ray excess at the Galactic center and a probable antiproton excess in the recent AMS-02 observation suggest that these two anomalies may be owing to the same origin—the dark matter (DM) annihilation into $b\bar{b}$, while these results seem in tension with the dwarf spheroidal galaxy observations. To give a compatible explanation about it, we consider the pseudoscalar DM particles $S_d^+S_d^-$ annihilating via $S_d^+S_d^- \to S_d^0S_d^0$, with the process mediated by a new scalar ϕ and S_d^0 quickly decaying into $b\bar{b}$. For the particles S_d^+, S_d^-, and S_d^0 in a triplet with degenerate masses, the annihilation cross section of DM today is linearly dependent on the relative velocity v_r, and thus constraints from the dwarf spheroidal galaxies are relaxed. The parameter spaces are derived with corresponding constraints. Though traces from the new sector seem challenging to be disclosed at the collider and in DM direct detections, the indirect search of the gamma-ray line from the S_d^0's decay has the potential to shed light on DM annihilations, with the energy of the gamma-ray line $\sim m_{S_d^0}/2$, i.e. about 50–75 GeV.

DOI: 10.1103/PhysRevD.96.055009

I. INTRODUCTION

Today the nature of dark matter (DM) is still unclear, and the cosmic ray observation may indirectly provide some properties of DM. One possible DM signature is the Galactic center (GC) 1–3 GeV gamma-ray excess, which may be due to the weakly interacting massive particle (WIMP)-type DM annihilating into $b\bar{b}$, $c\bar{c}$, $q\bar{q}$ (light quarks u, d, s), $\tau\bar{\tau}$ *et al.* [1–15], e.g., WIMPs in a mass range of about 35–74 GeV annihilating into $b\bar{b}$ with the cross section of about $(1\text{–}3)\times 10^{-26}$ cm^3/s. Meanwhile, the updated constraints of the dwarf spheroidal galaxies from the Fermi-LAT [16–18] seem in tension with most DM interpretations of the GC gamma-ray excess. Yet, some schemes can also be compatible with the constraints of dwarf galaxies, such as WIMPs annihilating into $\mu^+\mu^-$, e^+e^- [19,20], decays of the asymmetric DM with anti-DM holding enough energy to escape dwarf spheroidal galaxies [21], or the p-wave annihilating DM from a decaying predecessor [22]. Another possible explanation about the gamma-ray excess is the millisecond pulsars [2–4,23–27], while some discussions [28–31] indicate that this astrophysical explanation seems challenging to produce the majority of the observed gamma-ray excess.

In addition, the charged cosmic rays may also shed light on the properties of DM. Recently, the analysis of the antiproton flux from the AMS-02 observations [32] indicates the existence of a possible DM signal, e.g., WIMPs in a mass range of around 50–80 GeV annihilating into $b\bar{b}$ with the cross section of about $(1\text{–}5)\times 10^{-26}$ cm^3/s [33,34]. It happens that the range of DM inferred from the GC gamma-ray excess could coincide with that from antiproton observations, and these two messenger results suggest that the signals may be owing to the same origin from DM annihilations, i.e., WIMPs in a mass range of about 50–75 GeV mainly annihilating into $b\bar{b}$ with an annihilation cross section $\sim(1\text{–}3)\times 10^{-26}$ cm^3/s (this is corresponding to about a 2σ region for the two joint fitting results of Ref. [35]).

Now, how to realize the DM annihilations suggested above and meanwhile being compatible with constraints from dwarf spheroidal galaxies becomes a crucial question,[1] and this is of our concern in this paper. Here we try to relax the tension in the mechanism, and consider a scenario that DM pairs annihilate into pairs of unstable particles with the unstable particles mainly decaying into the standard model (SM) $b\bar{b}$. To satisfy the constraints from dwarf galaxies, a possible solution is DM and the unstable particle being in a multiplet with nearly degenerate masses. The annihilations of DM near the threshold are phase space suppressed today, which is sensitive to the velocity of DM (see, e.g., Refs. [37,38]), and the constraints from dwarf galaxies can be relaxed due to the relatively low velocity. This scheme can be realized via two dark charged pseudoscalar particles S_d^+, S_d^- and one neutral pseudoscalar particle S_d^0 being in a triplet (like SM pions) in the hidden sector (see, e.g., Ref. [38] for more). The DM candidate particles S_d^+, S_d^- are stable due to the dark charge, and the unstable neutral particle S_d^0 is considered to couple with SM

*jialb@mail.nankai.edu.cn

[1]In Ref. [36], the tension becomes relaxed with the assumption that the DM in dwarf spheroidal galaxies may be overestimated, and the similar case was also discussed in Ref. [35].

fermions with the couplings proportional to the fermions' masses. A new scalar field is introduced, which mediates the main annihilation process of DM $S_d^+ S_d^- \to S_d^0 S_d^0$. As the annihilation of DM today is suppressed, to obtain the indicated DM annihilation cross section, we consider the case of DM annihilating near the resonance. This scheme is also helpful to evade the present stringent constraints from DM direct detections [39–42].

For thermal freeze-out DM, the DM and SM particles were in the thermal equilibrium for some time in the early universe, and this can be easily realized for the case of DM directly annihilating into SM particles. For the DM annihilations of concern, the thermal equilibrium is obtained via a small mixing between the new scalar mediator and the SM Higgs boson. This sets a lower bound on the mixing, and the corresponding constraint will be derived. The possible traces from the hidden sector will be discussed, i.e., the production of the new scalar at the collider, indirect detections of the γ-ray line, and the search of DM in direct detections.

This work is organized as follows. After this introduction, we briefly give the interactions of new scalar mediated WIMPs in Sec. II. Next we will discuss the indicated WIMP annihilations in Sec. III. Then we give a numerical analysis about traces of the new sector with corresponding constraints in Sec. IV. The last section is a brief conclusion and discussion.

II. INTERACTIONS OF NEW SCALAR MEDIATED WIMPS

In this paper, we consider that two dark charged pseudoscalar particles S_d^+, S_d^- and one neutral pseudoscalar particle S_d^0 are in a dark triplet, with the stable particles S_d^+, S_d^- being DM candidates and the unstable particle S_d^0 decaying into SM fermions. This can be obtained under a gauge symmetry and/or a global symmetry, e.g., dark pions in the hidden sector SU(N) symmetry [38,43]. A new scalar field Φ is introduced which couples to the dark triplet particles, while the SM Higgs field H does not directly interact with the dark triplet particles. The effective interactions between Φ and S_d^+, S_d^-, S_d^0, H are taken as

$$\mathcal{L}_\Phi^i = -\frac{1}{2}\lambda\Phi^2 S_d^+ S_d^- - \frac{1}{4}\lambda_0\Phi^2 S_d^0 S_d^0 - \mu\Phi S_d^+ S_d^- - \frac{1}{2}\mu_0\Phi S_d^0 S_d^0 - \lambda_h\Phi^2\left(H^\dagger H - \frac{v^2}{2}\right) - \mu_h\Phi\left(H^\dagger H - \frac{v^2}{2}\right), \quad (1)$$

where $v \approx 246$ GeV is the vacuum expectation value, and Φ is taken to be no vacuum expectation gained [44,45]. The mass splitting Δ between S_d^+ and S_d^0 is $\Delta = m_{S_d^+} - m_{S_d^0}$, and this splitting can be very small due to the symmetry in the dark sector, i.e., $|\Delta| \ll m_{S_d^+}, m_{S_d^0}$. Here we take $\lambda_0 = \lambda$, $\mu_0 = \mu$ for simplicity. The neutral pseudoscalar S_d^0 couples to SM fermions, and the effective form is taken as

$$\mathcal{L}_S^i = \sum_f i g_f \bar{f}\gamma^5 f S_d^0, \quad (2)$$

with g_f being proportional to the fermion's mass.[2]

The Φ field mixes with the scalar component h' of the Higgs field after the electroweak symmetry breaking, generating the mass eigenstates ϕ, h in forms of

$$\begin{pmatrix}\phi\\ h\end{pmatrix} = \begin{bmatrix}\cos\theta & \sin\theta\\ -\sin\theta & \cos\theta\end{bmatrix}\begin{pmatrix}\Phi\\ h'\end{pmatrix}, \quad (3)$$

where θ is the mixing angle, with the value

$$\tan 2\theta = \frac{2v\mu_h}{m_\Phi^2 - m_{h'}^2}. \quad (4)$$

For the alteration of the Higgs sector being as small as possible, here we consider the case of $\lambda_h \ll 1$ and $|v\mu_h| \ll \min(m_{h'}^2, m_\Phi^2)$. Thus, one has $m_h \simeq m_{h'}$, $m_\phi \simeq m_\Phi$, and the mixing angle θ can be very small compared with unity, i.e., $|\sin\theta| \simeq |\theta| \ll 1$. In addition, the mixing angle can play a crucial role in the equilibrium between the DM sector and SM sector in the early universe, and this will be discussed in the following.

III. WIMP ANNIHILATIONS

Here the WIMP pair $S_d^+ S_d^-$ mainly annihilates into $S_d^0 S_d^0$ with the transition mediated by ϕ, and S_d^0 decays into SM massive fermions. The corresponding annihilation cross section in one particle rest frame is

$$\sigma_{ann} v_r \simeq \frac{1}{2}\frac{\beta_f}{32\pi(s - 2m_{S_d^+}^2)}\frac{\mu^4}{(s - m_\phi^2)^2 + m_\phi^2\Gamma_\phi^2}, \quad (5)$$

where v_r is the relative velocity between a WIMP pair, and the factor $\frac{1}{2}$ is due to the $S_d^+ S_d^-$ pair required in annihilations. s is the total invariant mass squared, and Γ_ϕ is the decay width of ϕ. β_f is a kinematic factor, with $\beta_f = \sqrt{1 - 4m_{S_d^0}^2/s}$. The annihilation of a WIMP pair near the threshold is deeply phase space suppressed today. To meet the annihilation cross section indicated by the GC gamma-ray excess and antiproton observations and meanwhile being compatible with the DM relic density (see Appendix A for the relic density calculations), we consider the WIMPs annihilating near the resonance. In the nonrelativistic case, we have $s \simeq 4m_{S_d^+}^2 + m_{S_d^+}^2 v_r^2$. The typical v_r of DM today in the Milky Way is $v_r/c \sim 10^{-3}$, and the value is $v_r/c \lesssim 10^{-4}$ in the dwarf galaxies. For WIMP annihilations today, the factor β_f can be approximately written as

[2]This effective coupling can be obtained, e.g., via interactions in the technicolor-like scheme [46–49].

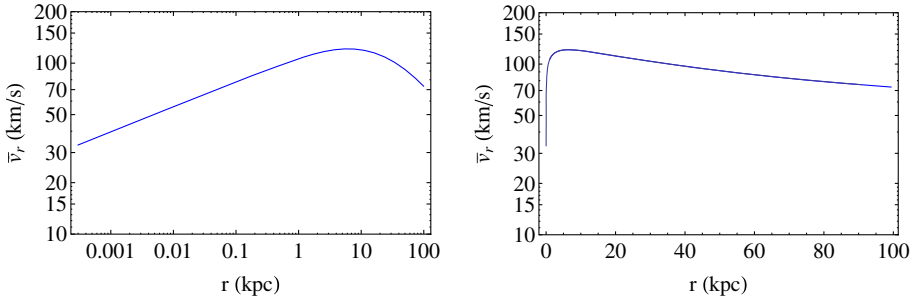

FIG. 1. The result of $\bar{v}_r$ as a function of r in the Milky Way.

$$\beta_f \approx \sqrt{2\frac{\Delta}{m_{S_d^+}} + \frac{1}{4}v_r^2}. \tag{6}$$

To be compatible with the constraints from dwarf galaxies, the constraint of the mass splitting is $|\Delta| \ll 10^{-7} m_{S_d^+}$, and thus the factor β_f is $\beta_f \approx |v_r|/2$ (see also Ref. [38]).

The WIMP pair annihilations today depend on the relative velocity v_r. In the Milky Way, the averaged relative velocity $\bar{v}_r$ as a function of r is shown in Fig. 1. For more details, see Appendix B. For a given position, the averaged annihilation cross section $\langle\sigma_{ann}v_r\rangle_0$ today can be obtained via Eq. (5), with β_f replaced by $\bar{\beta}_f$, and $\bar{\beta}_f \simeq |\bar{v}_r|/2$.

Now we turn to the GC gamma-ray excess via DM annihilations. In the Milky Way, for a solid angle $\Delta\Omega$, the differential flux of the photon $d\Phi_\gamma/dE_\gamma$ from DM annihilations can be written as

$$\frac{d\Phi_\gamma}{dE_\gamma} = \int_{\Delta\Omega}\int_{\text{l.o.s.}} \frac{dld\Omega'}{4\pi}\frac{\rho_{\text{DM}}^2\langle\sigma_{ann}v_r\rangle_0}{2m_{\text{DM}}^2}\frac{dN_\gamma}{dE_\gamma}. \tag{7}$$

When $\langle\sigma_{ann}v_r\rangle_0$ is insensitive to the DM velocity, a J-factor can be separated from Eq. (7), with the form

$$J = \int_{\Delta\Omega}\int_{\text{l.o.s.}} \rho_{\text{DM}}^2 dld\Omega'. \tag{8}$$

In this paper, due to $\bar{\beta}_f$, the averaged annihilation cross section of DM today is velocity dependent. Here, a weighted $\beta_J \simeq |v_J|/2$ is introduced, with

$$v_J = \frac{\int_{\Delta\Omega}\int_{\text{l.o.s.}} \bar{v}_r\rho_{\text{DM}}^2 dld\Omega'}{J}. \tag{9}$$

Thus, Eq. (7) can be rewritten as

$$\frac{d\Phi_\gamma}{dE_\gamma} = \frac{\langle\sigma_{ann}v_r\rangle_J}{8\pi m_{\text{DM}}^2}\frac{dN_\gamma}{dE_\gamma}J, \tag{10}$$

where $\langle\sigma_{ann}v_r\rangle_J$ is obtained via Eq. (5), with β_f replaced by β_J.

According to Eq. (10), to obtain the indicated DM annihilations, an alternative scheme is the WIMP pair annihilations via the process $S_d^+S_d^- \to S_d^0S_d^0 \to (b\bar{b})(b\bar{b})$. Here the WIMP mass is doubled compared with that in the Introduction, and the required annihilation cross section $\langle\sigma_{ann}v_r\rangle_J$ is multiplied by two, i.e., in a range of about

$$m_{S_d^+} \sim 100\text{–}150 \text{ GeV},$$
$$\langle\sigma_{ann}v_r\rangle_J \sim (2\text{–}6)\times 10^{-26} \text{ cm}^3/\text{s}.$$

This type DM annihilation is of our concern, and it is nearly equivalent to the indicated DM annihilations in the Introduction in kinematics.

Suppose that the distribution of the DM halo is spherical around the GC. For the gamma rays within a 5° cone towards the GC, the main contribution is from the region where the radius $r \lesssim 0.74$ kpc around the GC. Furthermore, it can be obtained that the distribution of Eq. (B3) is valid for $r \geq 3\times 10^{-4}$ kpc. The region of interest with 3×10^{-4} kpc $\leq r \lesssim 0.74$ kpc around the GC can give the main contribution to the 5° cone from the GC. Substituting the corresponding values, the value of v_J is obtained, with

$$v_J \approx 83 \text{ km/s}. \tag{11}$$

Meanwhile, the typical relative velocities in dwarf spheroidal galaxies are less than 15 km/s [22,50,51]. This means that the DM annihilation cross sections in dwarf spheroidal galaxies are just about (or less than) 1/5 of the $\langle\sigma_{ann}v_r\rangle_J$ value at the GC, i.e., the equivalent annihilation cross section (DM directly annihilating into $b\bar{b}$) $\lesssim(0.2\text{–}0.6)\times 10^{-26}$ cm^3/s. Thus, the constraints from dwarf spheroidal galaxies (Refs. [16–18]) are relaxed and compatible with the GC gamma-ray excess.

In addition, the indicated DM mass and annihilation cross section in the Introduction can give a joint fit to both the GC gamma-ray excess and the AMS-02 antiproton observations with the assumption of the same annihilation cross section (velocity independent). Here the annihilation cross section of DM is linearly dependent on the relative velocity. It can be seen from Fig. 1 that the typical $\bar{v}_r$ in the Milky Way is about 100 km/s, and thus the parameter space of the GC gamma-ray excess is consistent with the AMS-02 antiproton observations. Moreover, as a rough

estimate, a slightly larger typical DM annihilation cross section at significant regions (near the Sun) is also favored by the AMS-02 antiproton observations [33,34], and this suggests that the velocity linearly dependent DM annihilations could give a sightly better fit compared with the velocity independent case. Further explorations are needed about these types of DM annihilations.

Considering the annihilations of DM near the resonance, we note $\xi = m_\phi/2m_{S_d^+}$, and thus ξ is around 1. The form of Eq. (10) is feasible in the case of the relative velocity being negligible compared with the mass difference between m_ϕ and $2m_{S_d^+}$, i.e., $(v_J/c)^2 \ll 8|\xi - 1|$. According to Eq. (11), this is valid when

$$|\xi - 1| \gtrsim 10^{-7}. \tag{12}$$

In addition, the $\sin^2\theta$ should be small enough to keep the process $S_d^+ S_d^- \to S_d^0 S_d^0$ dominant in DM annihilations today. The main SM modes in DM annihilations are W^+W^-, Z^0Z^0 (hh may also be allowed), and these modes are away from the threshold. Note $\mu = km_{S_d^+}$. For the range of concern, considering Eqs. (5), (10), and (11), one has that the $\sin^2\theta$ should be approximately smaller than the value $5 \times 10^3 k^2/m_{S_d^+}^4(\mathrm{GeV})$, with $m_{S_d^+}$ in units of GeV. Here, the value

$$\sin^2\theta \lesssim 10^{-5}k^2\left(\frac{100}{m_{S_d^+}}\right)^4 \tag{13}$$

is adopted. When $\xi > 1$, to obtain the DM annihilations of concern, the required $\xi - 1$ is of order 10^{-7}. For the $|\xi - 1|$ value as large as possible within the parameter space, we focus on the case of $\xi < 1$ in the following. Moreover, for the case that the mass of the mediator m_ϕ is about twice of the DM mass, this behavior may be naturally realized in other contexts. For example, for the Kaluza-Klein (KK) particles in the universal extra dimension, the masses of the second level KK particles can be twice of the first level KK particles. Thus, pairs of the first level KK particles can annihilate closely to the resonance via the second level KK particles. For more discussions, see, e.g., Refs. [52,53].

IV. NUMERICAL ANALYSIS WITH CONSTRAINTS

Here we give a numerical analysis about the new sector beyond the SM. Some parameters are input as follows: $m_t = 173.21$ GeV, $m_b = 4.18$ GeV, $m_W = 80.385$ GeV, $m_Z = 91.1876$ GeV, $G_F = 1.1663787 \times 10^{-5}$ GeV^{-2} [54], and $m_h = 125.09$ GeV [55].

A. The results with the DM relic density

Here the values of the parameters μ, ξ will be evaluated with the constraint of the DM relic density. The DM relic density today is 0.1197 ± 0.0042 [56]. The DM annihilation cross section $\langle\sigma_{ann}v_r\rangle_J$ is sensitive to the value 1–ξ (here $\xi < 1$, as discussed above). For ξ in the range of Eq. (12), the decay width Γ_ϕ can be neglected in DM annihilations when Eq. (13) is satisfied. Taking the constraint from the DM relic density, the values of $\langle\sigma_{ann}v_r\rangle_J$, the coupling parameter k as a function of $1 - \xi$, are shown in Figs. 2 and 3, respectively, with $m_{S_d^+} = 100$ GeV, and 1–ξ varying from 10^{-5} to 10^{-3}. It can be seen that, when 1–ξ changes in a range of about $(0.45\text{–}1.0) \times 10^{-4}$, the $\langle\sigma_{ann}v_r\rangle_J$ varies from about 6×10^{-26} cm^3/s to 2×10^{-26} cm^3/s.

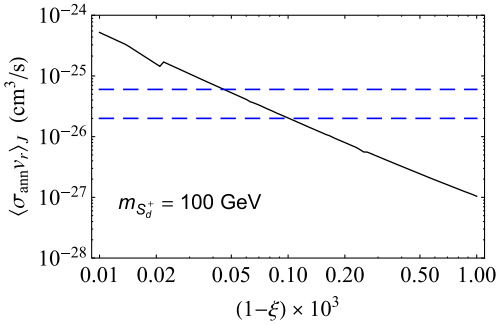

FIG. 2. The relation between $\langle\sigma_{ann}v_r\rangle_J$ and 1–ξ for $m_{S_d^+} = 100$ GeV. The value of 1–ξ varies in a range of $10^{-5} - 10^{-3}$, and the solid curve is the corresponding value of $\langle\sigma_{ann}v_r\rangle_J$ for a given 1–ξ. The upper dashed curve and the lower dashed curve are for the values of $\langle\sigma_{ann}v_r\rangle_J = 6 \times 10^{-26}$ cm^3/s and 2×10^{-26} cm^3/s respectively.

For a given 1–ξ, the value of $\langle\sigma_{ann}v_r\rangle_J$ is not sensitive to the mass $m_{S_d^+}$ in the WIMP mass range of concern. The result is shown in Fig. 4 with $(1\text{–}\xi) = 0.45 \times 10^{-4}$, 1.0×10^{-4}, and the corresponding coupling parameter k is shown in Fig. 5. For $m_{S_d^+}$ in a range of 100–150 GeV, when 1–ξ changes in a range of about $(0.45\text{–}1.0) \times 10^{-4}$, the $\langle\sigma_{ann}v_r\rangle_J$ varies from about 6×10^{-26} cm^3/s to 2×10^{-26} cm^3/s. This parameter range can give an explanation about the GC gamma-ray excess and the AMS-02 antiproton observations.

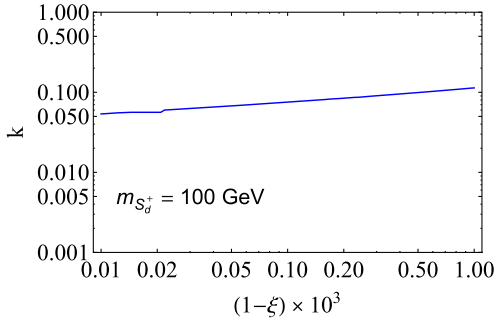

FIG. 3. The relation between k and 1–ξ for $m_{S_d^+} = 100$ GeV. The value of 1–ξ varies in a range of $10^{-5} - 10^{-3}$, and the solid curve is the corresponding value of k for a given 1–ξ.

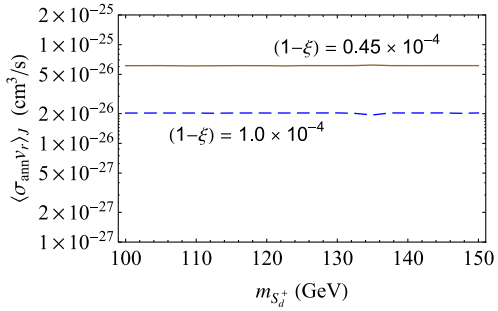

FIG. 4. The values of $\langle\sigma_{ann}v_r\rangle_J$ for two given values of $1-\xi$. The solid curve and dashed curve are corresponding to $(1-\xi) = 0.45\times10^{-4}$ and 1.0×10^{-4}, respectively. $m_{S_d^+}$ varies in a range of 100–150 GeV.

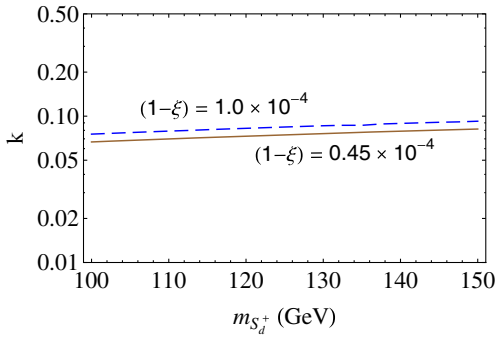

FIG. 5. The values of k for two given values of $1-\xi$. The solid curve and dashed curve are corresponding to $(1-\xi) = 0.45\times10^{-4}$ and 1.0×10^{-4}, respectively. $m_{S_d^+}$ varies in a range of 100–150 GeV.

B. The ϕ

1. The decay of ϕ and constraints from the collider

Because of a small mixing of ϕ with the SM Higgs boson, the couplings of ϕ with SM particles are Yukawa-type interactions. As discussed above, the mass of ϕ is about twice that of the DM mass, i.e., $m_\phi \sim 200$–300 GeV, and the mass m_ϕ being slightly below $2m_{S_d^+}$ is of our concern. In this case, the main decay products of ϕ are W^+W^-, Z^0Z^0. The decay width of $\phi \to VV$ $(V = W, Z)$ is

$$\Gamma_{\phi\to VV} \simeq \frac{G_F m_\phi^3 \sin^2\theta}{8\sqrt{2}\pi\delta_V}\sqrt{1-4y}(1-4y+12y^2), \quad (14)$$

with $y = m_V^2/m_\phi^2$, and $\delta_W = 1$, $\delta_Z = 2$. If $m_\phi > 250$ GeV, the channel $\phi \to hh$ is also allowed, and the decay width is

$$\Gamma_{\phi\to hh} \simeq \frac{G_F m_\phi^3 \sin^2\theta}{16\sqrt{2}\pi}\sqrt{1-\frac{4m_h^2}{m_\phi^2}}\left(1+\frac{2m_h^2}{m_\phi^2}\right)^2. \quad (15)$$

The branching ratios of the main decay channels of ϕ are shown in Fig. 6. For $m_\phi = 200$–300 GeV, the branching ratio $\mathcal{B}_{\phi\to ZZ}$ is about 20%–30%, and this channel can be tested at LHC. The production of ϕ at LHC is mainly through the gluon-gluon fusion, which is very similar to the same mass Higgs boson production, with the corresponding cross section multiplied by $\sin^2\theta$. For a pp collision at the center of mass energy $\sqrt{s}$ = a few TeV, the production cross section of Higgs with masses in a range of 200–300 GeV was estimated in Refs. [57,58]: at $\sqrt{s} = 13$ TeV, the cross section varies from about 17.5 pb ($m_h = 200$ GeV) to 9.5 pb ($m_h = 300$ GeV) and at $\sqrt{s} = 14$ TeV, the cross section varies from about 20.8 pb ($m_h = 200$ GeV) to 11.2 pb ($m_h = 300$ GeV). The search of high mass scalar resonance via the decay products of $Z^0Z^0 \to 4l$ $(l = e, \mu)$ at $\sqrt{s} = 13$ TeV was issued by the CMS [59] and ATLAS [60] Collaborations; i.e., the observed cross section is a few fb (with the branching ratios included). As a rough estimate, $\sin^2\theta \lesssim 10^{-2}$ is allowed by the search results. According to Eq. (13), the decay products of ϕ are buried in the messy background at LHC. Because of the suppression of $\sin^2\theta$, the search of ϕ is challenging in the future TeV scale e^+e^- collider, as indicated in Ref. [61].

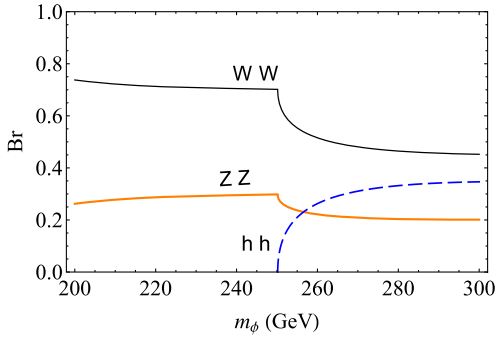

FIG. 6. The branching ratios of ϕ decaying into W^+W^-, Z^0Z^0 and hh.

2. The thermal equilibrium constraint

For thermal freeze-out WIMPs, the WIMPs and SM particles were in the thermal equilibrium in the early universe, i.e., the reaction rates of WIMPs ↔ SM particles should be over the expansion rate of the Universe for some time (see, e.g., Refs. [62–64] for more information) with

$$\langle\sigma v_r\rangle n_{\rm eq} \gtrsim 1.66\frac{\sqrt{g_*}T^2}{m_{\rm Pl}}, \quad (16)$$

where $n_{\rm eq}$ is the number density in the thermal equilibrium. In the relativistic limit, one has $n_f = 3\zeta(3)g_fT^3/4\pi^2$ for fermions, and $n_b = \zeta(3)g_bT^3/\pi^2$ for bosons. Here we consider the case that the reaction rate of SM particles → WIMPs can be over the expansion rate of the Universe at some time after the electroweak symmetry breaking. The transitions mainly contributed by the mixing between the

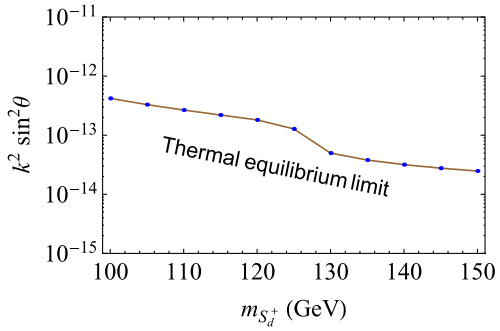

FIG. 7. The lower limit of $k^2 \sin^2\theta$ from the thermal equilibrium, with $m_{S_d^+}$ varying in a range of 100–150 GeV.

new scalar mediator and the Higgs boson. For details about the transitions, see Appendix C. Thus, Eq. (16) sets a lower bound on the mixing angle θ.

For the reaction rate, the annihilation cross section at least decreases as $1/s$ at a high energy, while the number density is exponentially suppressed at a low energy. In this paper $m_\phi \sim 2m_{S_d^+}$ and $m_{S_d^+} \sim 100$–150 GeV, as the transitions mediated by ϕ close to the resonance are significantly enhanced, we take the temperature scale $T \sim m_h$ and just consider the transitions mediated by ϕ with the contributions from W^+W^-, Z^0Z^0 and hh pairs in calculations. The lower limit of $k^2 \sin^2\theta$ is shown in Fig. 7.

C. The S_d^0

Here we assume that the lifetime of S_d^0 is less than (or similar to) the time scale from the beginning of the big bang to the moment that the temperature of the Universe is cooling to $m_{S_d^0}$, and thus S_d^0 is relativistic when its decay occurs. In this case, the number density of S_d^0 can be of its equilibrium value during S_d^+, S_d^- freeze out [38,65]. This sets a lower bound on the couplings of S_d^0 to SM fermions. In the early universe of the radiation dominant epoch, the temperature T can be written as a function of time t,

$$T = \left(\frac{16\pi^3}{45} G g_*\right)^{-1/4} t^{-1/2}, \tag{17}$$

where $G(= 1/m_{\rm Pl}^2)$ is the Newton's constant of gravitation. At $T \sim m_{S_d^0}$, the effective lifetime $\tau_{\rm eff}$ of S_d^0 is

$$\frac{1}{\tau_{\rm eff}} \simeq \frac{m_{S_d^0}}{\langle E_{S_d^0}\rangle} \sum_f \frac{g_f^2 N_c m_{S_d^0}}{8\pi} \sqrt{1 - 4m_f^2/m_{S_d^0}^2}, \tag{18}$$

where the time dilation effect is considered, and $\langle E_{S_d^0}\rangle$ is the averaged energy of S_d^0. At $T = m_{S_d^0}$, one has $\langle E_{S_d^0}\rangle \approx 3.25\, T$. The main decay product of S_d^0 is $b\bar{b}$, and thus we have

$$g_b^2 \gtrsim 7.40 \times 10^{-18} \sqrt{g_*} m_{S_d^0}({\rm GeV}). \tag{19}$$

The S_d^0 particle decays into $\gamma\gamma$ via charged fermion loops, and this is constrained by the GC gamma-ray line observation. The decay width is [66]

$$\Gamma_{S_d^0 \to \gamma\gamma} = \frac{\alpha^2 m_{S_d^0}^3}{256\pi^3} \left| \sum_f \frac{N_c Q_f^2 g_f F_{S_d^0}(\tau_f)}{m_f} \right|^2, \tag{20}$$

where $\tau_f = m_{S_d^0}^2/4m_f^2$, and

$$F_{S_d^0}(\tau_f) = \frac{2}{\tau_f} \times \begin{cases} \arcsin^2\sqrt{\tau_f}, & \tau_f \le 1 \\ -\frac{1}{4}\left[\log\frac{1+\sqrt{1-\tau_f^{-1}}}{1-\sqrt{1-\tau_f^{-1}}} - i\pi\right]^2, & \tau_f > 1 \end{cases}. \tag{21}$$

The top quark gives the main contribution to the decay width. Though the value of g_f is unknown, the branching ratio $\mathcal{B}_{S_d^0 \to \gamma\gamma}$ is set yet. Here, the annihilation cross section of the $\gamma\gamma$ is about $2\langle\sigma_{ann} v_r\rangle_J \times \mathcal{B}_{S_d^0 \to \gamma\gamma}$, with the energy of the gamma-ray line $\sim m_{S_d^0}/2$ (and also $\sim m_{S_d^+}/2$). The GC gamma-ray line was searched by the Fermi-LAT, and within 95% containment of the expectation value, no significant spectral line was found [67]. This limit can be employed to set an upper limit of about the DM annihilation of concern, and the revised upper limit can be obtained via the DM mass doubled and the corresponding upper limit multiplied by four compared with that in Ref. [67]. The result is shown in Fig. 8, and it can be seen that the gamma-ray line from DM annihilations is allowed by the present observations within 95% containment.

In addition, the S_d^0-like particle search at the collider can give an upper limit of about the coupling g_f, and here we give a brief discussion about it. For the S_d^0-b quark coupling, the constraints about g_b were discussed in Refs. [68,69], with $g_b \lesssim 0.1$, and this constraint is mild. Consider that the couplings of S_d^0 with SM fermions are smaller compared with that of the Higgs boson, and a limit $g_b^2 \lesssim 10^{-3}\sqrt{2} G_F m_b^2$ is taken here. This S_d^0-like particle is allowed by the diphoton observation at LHC [70].

D. DM direct detection

Now we turn to the direct detection of WIMPs. The WIMP-nucleon spin-independent elastic scattering mediated by h and ϕ is

$$\sigma_{\rm el} \simeq \frac{\sin^2\theta k^2 m_{S_d^+}^2 g_{hNN}^2 m_N^2}{4\pi(m_{S_d^+} + m_N)^2} \left(\frac{1}{m_h^2} - \frac{1}{m_\phi^2}\right)^2, \tag{22}$$

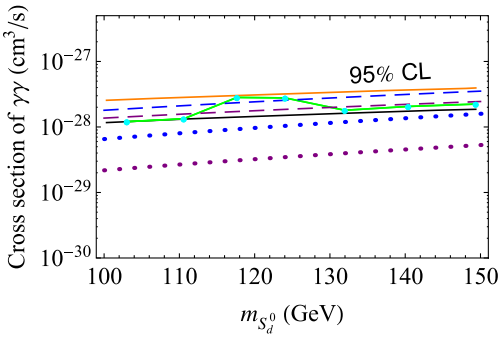

FIG. 8. The annihilation cross section of $\gamma\gamma$ (the value of $2\langle\sigma_{ann}v_r\rangle_J \times \mathcal{B}_{S_d^0\to\gamma\gamma}$), with the energy of the gamma-ray line $\sim m_{S_d^0}/2$ and $m_{S_d^0}$ varying in a range of 100–150 GeV. The lower dotted curve and upper dotted curve are for the case of $\langle\sigma_{ann}v_r\rangle_J = 2\times10^{-26}$ cm^3/s and 6×10^{-26} cm^3/s, respectively. The lower solid curve and upper solid curve are the expectation value of the gamma-ray line limit and the upper 95% containment of the expectation value, respectively, for the DM profile of NFWc R3 [67]. The two dashed curves are the expectation value of the gamma-ray line limit plus the contribution from DM annihilations, with the lower one and upper one for the case of $\langle\sigma_{ann}v_r\rangle_J = 2\times10^{-26}$ cm^3/s and 6×10^{-26} cm^3/s, respectively. The solid-dotted curve is the observed limit [67].

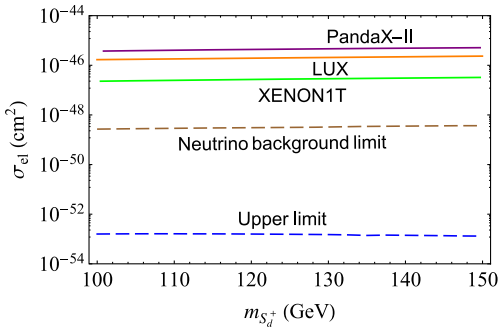

FIG. 9. The result of the elastic scattering cross section $\sigma_{\rm el}$. The solid curves from top to bottom are the upper limits set by DM direction detections of PandaX-II [41], LUX [42] and XENON1T [40]. The upper dashed curve and lower dashed curve are the lower detection limit set by the neutrino background [77] and the upper limit of the DM scattering from Eq. (13), respectively.

where m_N is the nucleon mass. g_{hNN} is the effective Higgs-nucleon coupling, and $g_{hNN} \simeq 1.1\times10^{-3}$ [71] is adopted here.[3]

The recent DM direct detections of XENON1T [40], PandaX-II [41], and LUX [42] set stringent constraints on WIMP-type DM. To obtain the upper limit of $\sigma_{\rm el}$, the value of k is taken for the case of $(1-\xi) = 1.0\times10^{-4}$ in Fig. 5. Considering the upper limit of Eq. (13), the result is shown in Fig. 9. The expected upper limit of the DM scattering is far below the neutrino background estimated in Ref. [77], and the DM of concern escapes the future direct detection experiments.

V. CONCLUSION AND DISCUSSION

In this paper, the DM annihilation of $S_d^+S_d^- \to S_d^0S_d^0$ mediated by ϕ with S_d^0 quickly decaying into $b\bar{b}$ has been studied to explain the GC gamma-ray excess and AMS-02 antiproton observations, with $m_{S_d^+}$ in a range of 100–150 GeV and the DM annihilation cross section $\langle\sigma_{ann}v_r\rangle_J = 2$–$6\times10^{-26}$ cm^3/s. In this scenario, the particles S_d^+, S_d^-, and S_d^0 are in a triplet in hidden sector with degenerate masses. The annihilation cross section of DM today is linearly dependent on the relative velocity v_r, and thus constraints from the dwarf spheroidal galaxies are suppressed and relaxed. With the indication of the GC gamma-ray excess, we consider the DM annihilating near the resonance, and the weighted relative velocity $v_J \approx 83$ km/s is derived.

The values of the coupling parameter k and the mass ratio parameter ξ are derived with the constraint of the DM relic density. In the DM mass range of concern, when 1–ξ varies in a range of $(0.45$–$1.0)\times10^{-4}$, the corresponding $\langle\sigma_{ann}v_r\rangle_J$ varies from about 6×10^{-26} cm^3/s to 2×10^{-26} cm^3/s. This is favored by the joint results of the GC gamma-ray excess and the AMS-02 antiprotons. In addition, by a rough estimate, it suggests that the velocity linearly dependent DM annihilations could give a sightly better fit compared with the usual assumption of velocity independent. Moreover, the case that the mass of the mediator is about twice of the DM mass, this may be related to other contexts, such as the universal extra dimension [52], or other undiscovered symmetries. Further explorations are needed for the velocity linearly dependent DM annihilations.

The upper limit of the mixing angle θ set by LHC is mild, and the search of ϕ particle is challenging at future collider experiments. An upper limit on the DM-nucleon elastic scattering cross section is set by the upper limit of θ from the DM main annihilation process $S_d^+S_d^- \to S_d^0S_d^0$, and this limit is far below the neutrino background in direct detections. The thermal equilibrium in the early Universe sets a lower limit on $k\sin\theta$, which has been calculated. Though traces from the new sector are difficult to be disclosed via the search at the collider and the DM direct detection, the indirect search of the gamma-ray line from S_d^0's decay has the potential to shed light on DM annihilations, with the energy of the gamma-ray line $\sim m_{S_d^0}/2$ (about 50–75 GeV). We look forward to more precise observations on the GC gamma-ray line, with the results from the Fermi-LAT [67], the Dark Matter Particle Explorer [78], the Cherenkov Telescope Array [79], the High Energy cosmic-Radiation Detection [80,81], and the GAMMA-400 [82,83].

[3]See, e.g., Refs. [72–76] for more.

ACKNOWLEDGMENTS

This work was supported by the National Natural Science Foundation of China under Contract No. 11505144, and the Research Fund for the Doctoral Program of the Southwest University of Science and Technology under Contract No. 15zx7102.

APPENDIX A: THE ABUNDANCE OF DM

The thermally averaged annihilation cross section of DM at temperature T is [84,85]

$$\langle\sigma_{ann}v_r\rangle = \frac{2x}{K_2^2(x)}\int_0^\infty d\varepsilon\sqrt{\varepsilon}(1+2\varepsilon) \times K_1(2x\sqrt{1+\varepsilon})\sigma_{ann}v_r, \tag{A1}$$

with $\varepsilon = (s-4m_{S_d^+}^2)/4m_{S_d^+}^2$, and $x = m_{S_d^+}/T$. K_i is the modified Bessel function of order i. For thermal freeze-out DM at temperature T_f, the thermally averaged annihilation cross section links to the DM relic density Ω_D today via the relation [86,87]

$$\Omega_D h^2 \simeq \frac{1.07\times10^9\ \mathrm{GeV}^{-1}}{J_{ann}\sqrt{g_*}m_{\mathrm{Pl}}}, \tag{A2}$$

with

$$J_{ann} = \int_{x_f}^\infty \frac{\langle\sigma_{ann}v_r\rangle}{x^2}dx, \tag{A3}$$

and the parameter x_f ($x_f = m_{S_d^+}/T_f$) can be approximately written as

$$x_f \simeq \ln 0.038\frac{gm_{\mathrm{Pl}}m_{S_d^+}\langle\sigma_{ann}v_r\rangle}{\sqrt{g_*x_f}}. \tag{A4}$$

Here h is the reduced Hubble constant (in units of 100 km s^{-1} Mpc^{-1}), and g_* is the effective number of the relativistic degrees of freedom at temperature T_f. m_{Pl} is the Planck mass with $m_{\mathrm{Pl}} = 1.22\times10^{19}$ GeV, and g is the degrees of freedom of DM. The value of x_f is about 20. Here the DM particles S_d^+, S_d^- are nonrelativistic when they freeze-out. In this paper, we consider the case that S_d^0 remains in thermal equilibrium with SM particles before $S_d^+S_d^-$ freeze-out,[4] as discussed in Refs. [38,89]. The abundances of S_d^+, S_d^-, and S_d^0 are nearly to be the equilibrium abundances before S_d^+, S_d^- freeze-out [38,65,89], and Eq. (A2) is available.

[4]For other case, see, e.g., discussions in Ref. [88].

APPENDIX B: THE RELATIVE VELOCITY

For a WIMP pair with velocities v_1, v_2 in the GC, dwarf spheroidal galaxies or the whole Milky Way, the averaged annihilation cross section today is

$$\langle\sigma_{ann}v_r\rangle_0 = \frac{1}{2}\int_0^{v_{\mathrm{esc}}}dv_1\int_0^{v_{\mathrm{esc}}}dv_2\int_{-1}^1 d\cos\theta f(v_1)f(v_2)\sigma_{ann}v_r, \tag{B1}$$

where the relative velocity v_r can be obtained via the relation $v_r = \sqrt{v_1^2+v_2^2-2v_1v_2\cos\theta}$. The escape velocity v_{esc} is radial position r dependent, and one has [90]

$$v_{\mathrm{esc}}^2 = 2\int_r^\infty\frac{dr}{r}v_c^2(r), \tag{B2}$$

with $v_c(r)$ being the circular velocity (see Refs. [91,92] for the value of v_c at a given r in the Milky Way). $f(v)$ is the velocity distribution, and here a Maxwell-Boltzmann distribution is adopted [22,90,93]

$$f(v) = \frac{3\sqrt{6}}{\sqrt{\pi}\sigma_v^3}v^2e^{-3v^2/2\sigma_v^2}, \tag{B3}$$

where σ_v is the velocity dispersion at a given r. For the Galactic DM, the fitting form is

$$\sigma_v^3(r) = v_0^3\left(\frac{r}{r_s}\right)^\chi\frac{\rho(r)}{\rho_0}, \tag{B4}$$

where $\chi = 1.64$ is adopted with the baryon contributions included [90], and $v_0 = 130$ km/s is taken [94,95]. A Navarro–Frenk–White (NFW) density profile of DM is adopted

$$\rho(r) = \frac{\rho_0}{(\frac{r}{r_s})^\gamma(1+\frac{r}{r_s})^{3-\gamma}}, \tag{B5}$$

with $r_s = 20$ kpc, and $\gamma = 1.2$ being adopted for the best fit result in Refs. [7,10]. The distance from the Sun to the GC is $R_\odot \simeq 8.5$ kpc, and ρ_0 is taken for the DM density near the Sun being $\sim$0.4 GeV/cm^3. An averaged $\bar{\beta}_f \simeq |\bar{v}_r|/2$ is introduced, with the averaged relative velocity

$$\bar{v}_r = \frac{1}{2}\int_0^{v_{\mathrm{esc}}}dv_1\int_0^{v_{\mathrm{esc}}}dv_2\int_{-1}^1 d\cos\theta f(v_1)f(v_2)v_r. \tag{B6}$$

APPENDIX C: THE TRANSITION OF SM → DM

Consider the ϕ mediated transitions of SM particles → WIMPs first. For each SM fermion species, the annihilation cross section is

$$\sigma v_r(f\bar{f}) = \frac{\lambda_{\rm SM}^2 \mu^2 (s-4m_f^2)}{32\pi(s-2m_f^2)} \frac{\sqrt{1-4m_{S_d^+}^2/s}}{(s-m_\phi^2)^2+m_\phi^2\Gamma_\phi^2}, \quad \text{(C1)}$$

with $\lambda_{\rm SM} = \sin\theta m_f(\sqrt{2}G_F)^{1/2}$. For the SM massive vector boson pair VV ($V = W, Z$), the annihilation cross section is

$$\sigma v_r(VV) = \frac{\sin^2\theta\mu^2\sqrt{2}G_F s^2}{144\pi(s-2m_V^2)} \frac{\sqrt{1-4m_{S_d^+}^2/s}}{(s-m_\phi^2)^2+m_\phi^2\Gamma_\phi^2} \times \left(1-\frac{4m_V^2}{s}+\frac{12m_V^4}{s^2}\right). \quad \text{(C2)}$$

For the hh pair, the annihilation cross section is

$$\sigma v_r(hh) = \frac{\sin^2\theta\mu^2\sqrt{2}G_F m_\phi^4}{16\pi(s-2m_h^2)} \frac{\sqrt{1-4m_{S_d^+}^2/s}}{(s-m_\phi^2)^2+m_\phi^2\Gamma_\phi^2} \times \left(1+\frac{2m_h^2}{m_\phi^2}\right)^2. \quad \text{(C3)}$$

The transitions mediated by h are similar to that of ϕ, just with m_ϕ, Γ_ϕ replaced by m_h, Γ_h, respectively. For a 125 GeV SM Higgs boson, the total width is $\Gamma_h = 4.07\times10^{-3}$ GeV [54,96].

[1] L. Goodenough and D. Hooper, Possible evidence for dark matter annihilation in the ynner Milky Way from the fermi gamma ray space telescope, arXiv:0910.2998.

[2] D. Hooper and L. Goodenough, Dark matter annihilation in the Galactic center as seen by the fermi gamma ray space telescope, Phys. Lett. B **697**, 412 (2011).

[3] D. Hooper and T. Linden, Origin of the gamma rays from the Galactic center, Phys. Rev. D **84**, 123005 (2011).

[4] K. N. Abazajian and M. Kaplinghat, Detection of a gamma-ray source in the Galactic center consistent with extended emission from dark matter annihilation and concentrated astrophysical emission, Phys. Rev. D **86**, 083511 (2012); Erratum, Phys. Rev. D **87**, 129902(E) (2013).

[5] D. Hooper, C. Kelso, and F. S. Queiroz, Stringent and robust constraints on the dark matter annihilation cross section from the region of the Galactic center, Astropart. Phys. **46**, 55 (2013).

[6] K. N. Abazajian, N. Canac, S. Horiuchi, and M. Kaplinghat, Astrophysical and dark matter interpretations of extended gamma-ray emission from the Galactic center, Phys. Rev. D **90**, 023526 (2014).

[7] T. Daylan, D. P. Finkbeiner, D. Hooper, T. Linden, S. K. N. Portillo, N. L. Rodd, and T. R. Slatyer, The characterization of the gamma-ray signal from the central Milky Way: A case for annihilating dark matter, Phys. Dark Universe **12**, 1 (2016).

[8] A. Alves, S. Profumo, F. S. Queiroz, and W. Shepherd, Effective field theory approach to the Galactic center gamma-ray excess, Phys. Rev. D **90**, 115003 (2014).

[9] B. Zhou, Y. F. Liang, X. Huang, X. Li, Y. Z. Fan, L. Feng, and J. Chang, GeV excess in the Milky Way: The role of diffuse galactic gamma-ray emission templates, Phys. Rev. D **91**, 123010 (2015).

[10] F. Calore, I. Cholis, and C. Weniger, Background model systematics for the fermi GeV excess, J. Cosmol. Astropart. Phys. 03 (2015) 038.

[11] P. Agrawal, B. Batell, P. J. Fox, and R. Harnik, WIMPs at the Galactic center, J. Cosmol. Astropart. Phys. 05 (2015) 011.

[12] F. Calore, I. Cholis, C. McCabe, and C. Weniger, A tale of tails: Dark matter interpretations of the Fermi GeV excess in light of background model systematics, Phys. Rev. D **91**, 063003 (2015).

[13] M. Ajello *et al.* (Fermi-LAT Collaboration), Fermi-LAT observations of high-energy γ-ray emission toward the Galactic center, Astrophys. J. **819**, 44 (2016).

[14] X. Huang, T. Enßlin, and M. Selig, Galactic dark matter search via phenomenological astrophysics modeling, J. Cosmol. Astropart. Phys. 04 (2016) 030.

[15] C. Karwin, S. Murgia, T. M. P. Tait, T. A. Porter, and P. Tanedo, Dark matter interpretation of the Fermi-LAT observation toward the Galactic center, Phys. Rev. D **95**, 103005 (2017).

[16] M. Ackermann *et al.* (Fermi-LAT Collaboration), Searching for Dark Matter Annihilation from Milky Way Dwarf Spheroidal Galaxies with Six Years of Fermi Large Area Telescope Data, Phys. Rev. Lett. **115**, 231301 (2015).

[17] S. Li, Y.-F. Liang, K.-K. Duan, Z.-Q. Shen, X. Huang, X. Li, Y.-Z. Fan, N.-H. Liao, L. Feng, and J. Chang, Search for gamma-ray emission from eight dwarf spheroidal galaxy candidates discovered in year two of Dark Energy Survey with Fermi-LAT data, Phys. Rev. D **93**, 043518 (2016).

[18] A. Albert *et al.* (Fermi-LAT and DES Collaborations), Searching for dark matter annihilation in recently discovered Milky Way satellites with Fermi-LAT, Astrophys. J. **834**, 110 (2017).

[19] J. Liu, N. Weiner, and W. Xue, Signals of a light dark force in the Galactic center, J. High Energy Phys. 08 (2015) 050.

[20] M. Kaplinghat, T. Linden, and H. B. Yu, Galactic Center Excess in γ Rays from Annihilation of Self-Interacting Dark Matter, Phys. Rev. Lett. **114**, 211303 (2015).

[21] E. Hardy, R. Lasenby, and J. Unwin, Annihilation signals from asymmetric dark matter, J. High Energy Phys. 07 (2014) 049.

[22] J. Choquette, J. M. Cline, and J. M. Cornell, p-wave annihilating dark matter from a decaying predecessor and the Galactic center excess, Phys. Rev. D **94**, 015018 (2016).

[23] K. N. Abazajian, The consistency of Fermi-LAT observations of the Galactic center with a millisecond pulsar

population in the central stellar cluster, J. Cosmol. Astropart. Phys. 03 (2011) 010.
[24] R. S. Wharton, S. Chatterjee, J. M. Cordes, J. S. Deneva, and T. J. W. Lazio, Multiwavelength constraints on pulsar populations in the Galactic center, Astrophys. J. **753**, 108 (2012).
[25] R. M. O'Leary, M. D. Kistler, M. Kerr, and J. Dexter, Young pulsars and the Galactic center GeV Gamma-ray excess, arXiv:1504.02477.
[26] R. Bartels, S. Krishnamurthy, and C. Weniger, Strong Support for the Millisecond Pulsar Origin of the Galactic Center GeV Excess, Phys. Rev. Lett. **116**, 051102 (2016).
[27] S. K. Lee, M. Lisanti, B. R. Safdi, T. R. Slatyer, and W. Xue, Evidence for Unresolved γ-Ray Point Sources in the Inner Galaxy, Phys. Rev. Lett. **116**, 051103 (2016).
[28] I. Cholis, D. Hooper, and T. Linden, Challenges in explaining the Galactic center Gamma-ray excess with millisecond pulsars, J. Cosmol. Astropart. Phys. 06 (2015) 043.
[29] T. Linden, Known radio pulsars do not contribute to the Galactic center gamma-ray excess, Phys. Rev. D **93**, 063003 (2016).
[30] D. Hooper and T. Linden, The gamma-ray pulsar population of globular clusters: implications for the gev excess, J. Cosmol. Astropart. Phys. 08 (2016) 018.
[31] D. Haggard, C. Heinke, D. Hooper, and T. Linden, Low mass X-ray binaries in the inner galaxy: Implications for millisecond pulsars and the GeV excess, J. Cosmol. Astropart. Phys. 05 (2017) 056.
[32] M. Aguilar *et al.* (AMS Collaboration), Antiproton Flux, Antiproton-to-Proton Flux Ratio, and Properties of Elementary Particle Fluxes in Primary Cosmic Rays Measured with the Alpha Magnetic Spectrometer on the International Space Station, Phys. Rev. Lett. **117**, 091103 (2016).
[33] A. Cuoco, M. Krämer, and M. Korsmeier, Novel Dark Matter Constraints from Antiprotons in the Light of AMS-02, Phys. Rev. Lett. **118**, 191102 (2017).
[34] M. Y. Cui, Q. Yuan, Y. L. S. Tsai, and Y. Z. Fan, Possible Dark Matter Annihilation Signal in the AMS-02 Antiproton Data, Phys. Rev. Lett. **118**, 191101 (2017).
[35] A. Cuoco, J. Heisig, M. Korsmeier, and M. Krämer, Probing dark matter annihilation in the Galaxy with antiprotons and gamma rays, arXiv:1704.08258.
[36] J. M. Cline, J. M. Cornell, D. London, and R. Watanabe, Hidden sector explanation of B-decay and cosmic ray anomalies, Phys. Rev. D **95**, 095015 (2017).
[37] L. B. Jia, Study of WIMP annihilations into a pair of on-shell scalar mediators, Phys. Rev. D **94**, 095028 (2016).
[38] J. Kopp, J. Liu, T. R. Slatyer, X. P. Wang, and W. Xue, Impeded dark matter, J. High Energy Phys. 12 (2016) 033.
[39] D. S. Akerib *et al.* (LUX Collaboration), Improved Limits on Scattering of Weakly Interacting Massive Particles from Reanalysis of 2013 LUX Data, Phys. Rev. Lett. **116**, 161301 (2016).
[40] E. Aprile *et al.* (XENON Collaboration), Physics reach of the XENON1T dark matter experiment, J. Cosmol. Astropart. Phys. 04 (2016) 027.
[41] A. Tan *et al.* (PandaX-II Collaboration), Dark Matter Results from First 98.7 Days of Data from the PandaX-II Experiment, Phys. Rev. Lett. **117**, 121303 (2016).
[42] D. S. Akerib *et al.* (LUX Collaboration), Results from a Search for Dark Matter in the Complete LUX Exposure, Phys. Rev. Lett. **118**, 021303 (2017).
[43] S. Bhattacharya, B. Melić, and J. Wudka, Pionic dark matter, J. High Energy Phys. 02 (2014) 115.
[44] M. Pospelov, A. Ritz, and M. B. Voloshin, Secluded WIMP dark matter, Phys. Lett. B **662**, 53 (2008).
[45] B. Batell, D. McKeen, and M. Pospelov, Singlet neighbors of the Higgs boson, J. High Energy Phys. 10 (2012) 104.
[46] S. Weinberg, Implications of dynamical symmetry breaking, Phys. Rev. D **13**, 974 (1976); Implications of dynamical symmetry breaking: An addendum, Phys. Rev. D **19**, 1277 (1979).
[47] L. Susskind, Dynamics of spontaneous symmetry breaking in the Weinberg-Salam theory, Phys. Rev. D **20**, 2619 (1979).
[48] E. Farhi and L. Susskind, Technicolor, Phys. Rep. **74**, 277 (1981).
[49] T. A. Ryttov and F. Sannino, Ultra minimal technicolor and its dark matter TIMP, Phys. Rev. D **78**, 115010 (2008).
[50] M. G. Walker, M. Mateo, E. W. Olszewski, O. Y. Gnedin, X. Wang, B. Sen, and M. Woodroofe, Velocity dispersion profiles of seven dwarf spheroidal galaxies, Astrophys. J. **667**, L53 (2007).
[51] Y. Zhao, X. J. Bi, H. Y. Jia, and P. F. Yin, and F. R. Zhu, Constraint on the velocity dependent dark matter annihilation cross section from Fermi-LAT observations of dwarf galaxies, Phys. Rev. D **93**, 083513 (2016).
[52] M. Kakizaki, S. Matsumoto, Y. Sato, and M. Senami, Significant effects of second Kaluza-Klein particles on dark matter physics, Phys. Rev. D **71**, 123522 (2005).
[53] M. Ibe, H. Murayama, and T. T. Yanagida, Breit-Wigner enhancement of dark matter annihilation, Phys. Rev. D **79**, 095009 (2009).
[54] C. Patrignani *et al.* (Particle Data Group), Review of particle physics, Chin. Phys. C **40**, 100001 (2016).
[55] G. Aad *et al.* (ATLAS and CMS Collaborations), Combined Measurement of the Higgs Boson Mass in pp Collisions at $\sqrt{s} = 7$ and 8 TeV with the ATLAS and CMS Experiments, Phys. Rev. Lett. **114**, 191803 (2015).
[56] P. A. R. Ade *et al.* (Planck Collaboration), Planck 2015 results. XIII. Cosmological parameters, Astron. Astrophys. **594**, A13 (2016).
[57] J. Baglio and A. Djouadi, Higgs production at the LHC, J. High Energy Phys. 03 (2011) 055.
[58] J. Ellis, Topics in Higgs physics, arXiv:1702.05436.
[59] CMS Collaboration, Report No. CMS-PAS-HIG-16-033.
[60] ATLAS Collaboration, Report No. ATLAS-CONF-2016-079.
[61] A. Djouadi, The anatomy of electroweak symmetry breaking. I. The Higgs boson in the standard model, Phys. Rep. **457**, 1 (2008).
[62] X. Chu, T. Hambye, and M. H. G. Tytgat, The four basic ways of creating dark matter through a portal, J. Cosmol. Astropart. Phys. 05 (2012) 034.
[63] M. J. Dolan, F. Kahlhoefer, C. McCabe, and K. Schmidt-Hoberg, A taste of dark matter: Flavour constraints on pseudoscalar mediators, J. High Energy Phys. 03 (2015) 171; Erratum, J. High Energy Phys. 07 (2015) 103(E).

[64] G. Krnjaic, Probing light thermal dark-matter with a Higgs portal mediator, Phys. Rev. D **94**, 073009 (2016).
[65] M. Kawasaki, G. Steigman, and H. S. Kang, Cosmological evolution of an early decaying particle, Nucl. Phys. **B403**, 671 (1993).
[66] A. Djouadi, The Anatomy of electro-weak symmetry breaking. II. The Higgs bosons in the minimal supersymmetric model, Phys. Rep. **459**, 1 (2008).
[67] M. Ackermann *et al.* (Fermi-LAT Collaboration), Updated search for spectral lines from Galactic dark matter interactions with pass 8 data from the Fermi Large Area Telescope, Phys. Rev. D **91**, 122002 (2015).
[68] A. Berlin, S. Gori, T. Lin, and L. T. Wang, Pseudoscalar portal dark matter, Phys. Rev. D **92**, 015005 (2015).
[69] J. Fan, S. M. Koushiappas, and G. Landsberg, Pseudoscalar portal dark matter and new signatures of vector-like fermions, J. High Energy Phys. 01 (2016) 111.
[70] G. Aad *et al.* (ATLAS Collaboration), Measurement of Higgs boson production in the diphoton decay channel in pp collisions at center-of-mass energies of 7 and 8 TeV with the ATLAS detector, Phys. Rev. D **90**, 112015 (2014).
[71] H. Y. Cheng and C. W. Chiang, Revisiting scalar and pseudoscalar couplings with nucleons, J. High Energy Phys. 07 (2012) 009.
[72] J. R. Ellis, A. Ferstl, and K. A. Olive, Reevaluation of the elastic scattering of supersymmetric dark matter, Phys. Lett. B **481**, 304 (2000).
[73] P. Gondolo, J. Edsjo, P. Ullio, L. Bergstrom, M. Schelke, and E. A. Baltz, DarkSUSY: Computing supersymmetric dark matter properties numerically, J. Cosmol. Astropart. Phys. 07 (2004) 008.
[74] X. G. He, T. Li, X. Q. Li, J. Tandean, and H. C. Tsai, Constraints on scalar dark matter from direct experimental searches, Phys. Rev. D **79**, 023521 (2009).
[75] J. M. Alarcon, J. Martin Camalich, and J. A. Oller, The chiral representation of the πN scattering amplitude and the pion-nucleon sigma term, Phys. Rev. D **85**, 051503 (2012).
[76] J. M. Cline, K. Kainulainen, P. Scott, and C. Weniger, Update on scalar singlet dark matter, Phys. Rev. D **88**, 055025 (2013); Erratum, Phys. Rev. D **92**, 039906(E) (2015).
[77] J. Billard, L. Strigari, and E. Figueroa-Feliciano, Implication of neutrino backgrounds on the reach of next generation dark matter direct detection experiments, Phys. Rev. D **89**, 023524 (2014).
[78] J. Chang, Dark matter particle explorer: The first chinese cosmic ray and hard γ-ray detector in space, Chin. J. Spac. Sci. **34**, 550 (2014).
[79] B. S. Acharya *et al.* (CTA Consortium), Introducing the CTA concept, Astropart. Phys. **43**, 3 (2013).
[80] S. N. Zhang *et al.* (HERD Collaboration), The high energy cosmic-radiation detection (HERD) facility onboard China's space station, Proc. SPIE Int. Soc. Opt. Eng. **9144**, 91440X (2014).
[81] X. Huang *et al.*, Perspective of monochromatic gamma-ray line detection with the High Energy cosmic-Radiation Detection (HERD) facility onboard China's space station, Astropart. Phys. **78**, 35 (2016).
[82] A. M. Galper *et al.*, Status of the GAMMA-400 project, Adv. Space Res. **51**, 297 (2013).
[83] N. P. Topchiev *et al.*, High-energy gamma-ray studying with GAMMA-400 after Fermi-LAT, J. Phys. Conf. Ser. **798**, 012011 (2017).
[84] P. Gondolo and G. Gelmini, Cosmic abundances of stable particles: Improved analysis, Nucl. Phys. **B360**, 145 (1991).
[85] M. Cannoni, Relativistic $\langle \sigma v_{\rm rel} \rangle$ in the calculation of relics abundances: A closer look, Phys. Rev. D **89**, 103533 (2014).
[86] E. W. Kolb and M. S. Turner, *The Early Universe* (Westview Press, Boulder, CO, 1994).
[87] K. Griest and D. Seckel, Three exceptions in the calculation of relic abundances, Phys. Rev. D **43**, 3191 (1991).
[88] J. A. Dror, E. Kuflik, and W. H. Ng, Codecaying Dark Matter, Phys. Rev. Lett. **117**, 211801 (2016).
[89] R. T. D'Agnolo and J. T. Ruderman, Light Dark Matter from Forbidden Channels, Phys. Rev. Lett. **115**, 061301 (2015).
[90] M. Cirelli and J. M. Cline, Can multistate dark matter annihilation explain the high-energy cosmic ray lepton anomalies?, Phys. Rev. D **82**, 023503 (2010).
[91] Y. Sofue and V. Rubin, Rotation curves of spiral galaxies, Annu. Rev. Astron. Astrophys. **39**, 137 (2001).
[92] Y. Sofue, Rotation curve and mass distribution in the Galactic center: From black fole to entire galaxy, Publ. Astron. Soc. Jpn. **65**, 118 (2013).
[93] B. Robertson and A. Zentner, Dark matter annihilation rates with velocity-dependent annihilation cross sections, Phys. Rev. D **79**, 083525 (2009).
[94] G. Battaglia, A. Helmi, H. Morrison, P. Harding, E. W. Olszewski, M. Mateo, K. C. Freeman, J. Norris, and S. A. Shectman, The radial velocity dispersion profile of the Galactic halo: Constraining the density profile of the dark halo of the Milky Way, Mon. Not. R. Astron. Soc. **364**, 433 (2005); Erratum, Mon. Not. R. Astron. Soc. **370**, 1055 (2006).
[95] W. Dehnen, D. McLaughlin, and J. Sachania, The velocity dispersion and mass profile of the Milky Way, Mon. Not. R. Astron. Soc. **369**, 1688 (2006).
[96] A. Denner, S. Heinemeyer, I. Puljak, D. Rebuzzi, and M. Spira, Standard model Higgs-boson branching ratios with uncertainties, Eur. Phys. J. C **71**, 1753 (2011).